

Article

Study on Gas Invasion Behavior of Gas–Liquid Displacement in Fractured Reservoirs

Cheng Ye ¹, Jiaqin Gong ¹, Kecheng Liu ¹, Jingjing Pei ¹, Shengjiang Xu ¹ and Peng Xu ^{2,*}¹ PetroChina Xinjiang Oilfield Engineering Technology Research Institute, Karamay 834000, China² School of Petroleum Engineering, Yangtze University, Wuhan 430100, China

* Correspondence: cdxupeng@yangtzeu.edu.cn

Abstract: When drilling or exploiting fractured formations, gas fluid displacement and invasion often occur, and gas invasion is very subtle and difficult to find. The gas in the fracture enters the wellbore and arrives near the wellhead with the drilling fluid. Improper treatment may lead to serious accidents such as lost circulation and blowout. In this study, using computational fluid dynamics (CFD) simulation software for modeling and grid generation, based on the volume of fluid (VOF) method, the gas invasion behavior under different conditions was simulated to explore the flow process and characteristics of gas invasion, and the effects of different drilling fluid properties and fracture morphology on gas invasion were analyzed. The experimental results show that the drilling fluid enters the fracture to compress the gas, making the pressure in the fracture greater than that in the wellbore, thus leading to the occurrence of gas invasion. The viscosity and density of the drilling fluid have different effects on the gas invasion process. The higher the viscosity, the smaller the possibility of gas invasion. However, when the viscosity of the drilling fluid gradually increases from 10–50 MPa·s, the change of gas invasion rate is small, all within 1.0–1.2 m/s. The higher the density, the more conducive to the occurrence of gas invasion. The inlet pressure has no obvious effect on the occurrence of gas invasion, and the occurrence time of the gas invasion fluctuates in 0.35 s at 0.5–2.5 MPa. With the increase in the fracture width and length, the possibility of gas invasion decreases, but there is an extreme value for the fracture height. The time of gas invasion does not change beyond this extreme value. When the fracture height is 100–700 mm, the time of gas invasion increases with the increase in the height; when the height is 700–900 mm, the gas invasion time does not change. These results provide a practical and effective method for enhancing oil recovery, preventing and treating gas invasion in gas–liquid flooding.

Keywords: gas invasion; gas–liquid displacement; gas–liquid two-phase flow; fracture; CFD simulation



Citation: Ye, C.; Gong, J.; Liu, K.; Pei, J.; Xu, S.; Xu, P. Study on Gas Invasion Behavior of Gas–Liquid Displacement in Fractured Reservoirs. *Processes* **2022**, *10*, 2533. <https://doi.org/10.3390/pr10122533>

Academic Editors: Tao Zhang, Zheng Sun, Dong Feng, Hung Vo Thanh and Wen Zhao

Received: 2 November 2022

Accepted: 25 November 2022

Published: 29 November 2022

Publisher's Note: MDPI stays neutral with regard to jurisdictional claims in published maps and institutional affiliations.



Copyright: © 2022 by the authors. Licensee MDPI, Basel, Switzerland. This article is an open access article distributed under the terms and conditions of the Creative Commons Attribution (CC BY) license (<https://creativecommons.org/licenses/by/4.0/>).

1. Introduction

In the process of oil and gas exploration drilling, when drilling multi-fracture and multi-cave formations, the drilling fluid will leak, and the gas in the formation will invade the wellbore [1]. When the drilling fluid is oil-based, under a certain pressure and temperature, the gas will dissolve in the oil-based drilling fluid to form dissolved gas, which is not easy to find in the early overflow detection [2,3]. When it rises to the wellhead, it can easily cause blowout and other accidents, reducing the oil and gas recovery rate. When the drilling fluid is water-based, the ground overflow monitoring is obvious, and the gas will slide and expand when entering the wellbore, and the upper overshoes may be damaged if the well is shut in for a long time [4–7]. The invasion of drilling fluid gas not only brings difficulties to drilling engineering, but also causes casualties and economic losses [8–15]. In recent years, scholars at home and abroad have also conducted a lot of research on the problem of gas invasion in fractured gas reservoirs. In order to reduce the harm caused by gas invasion, it is integral to systematically study the occurrence conditions,

mechanism, influencing factors, and prevention measures of gas invasion in gas–liquid displacement [16–18].

It is generally believed that gas invasion will occur when the local formation pressure is higher than the wellbore pressure. However, in the process of drilling, when the bottom hole is in a positive differential pressure state, gas invasion will also occur [19]. Beenion [20] analyzed and studied the drilling and completion process of a fractured gas reservoir. The research results show that in fractured formations, drilling fluid leakage and gas invasion can easily occur under negative pressure due to the difference in the density of the gas and the liquid, that is, blowout and leakage occur simultaneously. Nickens [21] considered the effects of pump speed, formation gas invasion, blowout preventer, throttle valve closing, and throttle valve adjustment. During gas invasion, the model can predict the change of flow rate and pressure with time and wellbore location. Zhang [22] assumed that gas invasion in gas–liquid displacement occurred at the bottom of the well, determining the gas invasion rate. The process of gas invasion from gas–liquid displacement to underbalanced gas invasion was studied. Zhang [23] assumed that the gas invasion occurred at the bottom hole during gas–liquid displacement and measured the gas invasion rate. The process of gas invasion from gas–liquid displacement to under equilibrium gas invasion is studied. Hou [24] simulated a real fracture by establishing a fracture space, and carried out visual experimental research on the gas invasion of gas–liquid displacement according to the gas–liquid displacement mechanism of fracture formation. On the basis of analyzing the reservoir geological characteristics of Shunnan Block in the northern slope of Tazhong, Fang [25] established a gas invasion model for gas–liquid displacement, simulated the gas invasion process of gas–liquid displacement with fluid computing software, and analyzed the main factors affecting the gas invasion of gas–liquid displacement [26].

The gas–liquid displacement invasion is a typical gas–liquid two-phase flow, which is very complicated in calculation, and it is difficult to observe the state of gas invasion intuitively in the laboratory. In this paper, Ansys Fluent is used for numerical simulation, the VOF multiphase flow model is used based on volume fraction equation and momentum equation (referring to the official instruction manual: https://ansyshelp.ansys.com/account/secured?returnurl=/Views/Secured/prod_page.html?pn=Fluent&pid=Fluent&lang=en&prodver=22, accessed on 10 September 2022), the gas invasion behavior of gas–liquid displacement is studied, and the effects of drilling fluid viscosity, density, fracture inlet pressure, fracture width, fracture height, and fracture length on gas invasion are discussed. In order to improve the safety of exploiting fractured gas reservoirs and increase the oil and gas recovery rate, it is necessary to clarify the influencing factors of gas invasion in gas–liquid displacement and the state characteristics of gas invasion.

2. Mathematical Model of Gas–Liquid Two-Phase Flow

There are many calculation models that can be used to calculate multi-phase flow problems in fluid, and selecting an appropriate calculation model is crucial to the final simulation results. The paper uses the volume of fluid (VOF) model, which is mainly used to track the interface position of two or more incompatible fluids. In the VOF model, the interface tracking is completed by solving the phase continuity equation, and the location of the interface is determined by finding the sharp change points in the volume component. The momentum equation of the mixed fluid is solved by the material properties of the mixed material, so the material properties of the mixed fluid will have sudden changes at the interface. The VOF model is mainly applied to the simulation of stratified flow, free surface flow, sloshing, flow with large bubbles in the liquid, dam break, and other phenomena. It can calculate the space–time distribution of the interface in the flow process. In the VOF model, the phases are completely independent, and there is no mutual penetration between them. The sum of the volume fractions of the phases is 1 in each governing equation. Therefore, if the volume fraction of the q phase is expressed by V_q , then V_{q0} indicates that there is no q phase in the control volume; V_{q1} indicates that the unit is full of q ; $0 < V_q < 1$ indicates that the q phase and one or more other phases are included in the control volume.

2.1. Volume Fraction Equation

In the VOF model, the interphase interface can be located by solving the mass equation for the volume fraction of multi-phase flow. For the q th phase, the volume fraction expression is shown in the formula:

$$\frac{\partial \alpha_q}{\partial t} + v_q \times \alpha_q = \frac{S_{\pm q}}{\rho_q} + \frac{1}{\rho_q} \sum_{p=1}^n (m_{pq} - m_{qp}) \quad (1)$$

where v_q is the velocity of the q th phase, α_q is the volume fraction of the q th phase, S_{aq} is the source phase of the q th phase, m_{pq} is the mass transfer from the p phase to the q phase, and m_{qp} is the mass transfer from the q phase to the p phase. It should be noted that the above equation is not the solution of the main phase, and the solution of the volume fraction of the main phase is as follows:

$$\sum_{p=1}^n \alpha_p = 1 \quad (2)$$

The attribute is determined by the phase separation of different control bodies in the flow field. In the two-phase system, if the subscripts c and d are used to express, and the volume fraction of the second phase is located and tracked, the density expression in each unit is as follows:

$$\rho = \alpha_d \rho_d + (1 - \alpha_d) \rho_c \quad (3)$$

In general, for the n -phase system, the average density of the volume fraction is as follows:

$$\rho = \sum \alpha_q \rho_q \quad (4)$$

Other properties, such as viscosity, are calculated in the same way [27,28].

2.2. Liquid-Phase Control Equation

In the process of gas invasion, the fluid flow at the junction of the fracture and wellbore changes from single-phase flow to gas–liquid two-phase flow, and follows the gas–liquid continuous phase equation and momentum equation. The continuity equation of the liquid phase is shown in the formula:

$$\frac{\partial}{\partial t} [\rho_m (1 - \gamma)] + \frac{\partial}{\partial z} [\rho_m v_m (1 - \gamma)] = 0 \quad (5)$$

where ρ_m is the density of the drilling fluid, kg/m^3 ; v_m is the drilling fluid velocity, m/s ; γ is the gas content, dimensionless [29].

2.3. Gas–Liquid Two-Phase Momentum Equation

In the interface between the gas phase and the liquid phase, the mass exchange phase will appear in the mass conservation equation of the gas phase and liquid phase. The following is the equation set describing the gas–liquid two-phase flow in the wellbore:

$$\frac{\partial}{\partial t} [\rho_m (1 - \gamma) + \rho_g v_g \gamma] + \frac{\partial}{\partial z} [\rho_m v_m^2 (1 - \gamma) + \rho_g \rho_g^2 \gamma] + \frac{\partial P}{\partial z} + \frac{\tau_0 P}{A} + [\rho_m (1 - \gamma) + \rho_g \gamma] g = 0 \quad (6)$$

where ρ_g is the gas density, kg/m^3 ; v_g is the real gas velocity, m/s ; P is the node pressure, MPa ; τ_0 is the shear force between the fluid and the pipe wall, N/m^2 .

2.4. Physical Model

There are many fractures and caves in the underground reservoir, providing huge storage space for natural gas and oil. When this formation is encountered during drilling, under the conditions of near balance and over balance, the annulus drilling fluid enters

the fracture under the action of differential pressure, compressing the gas in the fracture, causing the gas pressure in the fracture to increase. When the gas pressure in the fracture is greater than the hydrostatic fluid column pressure in the wellbore, local negative pressure will be generated between the two, causing gas invasion into the wellbore. The physical model is shown in Figure 1, and the parameters are shown in Table 1.

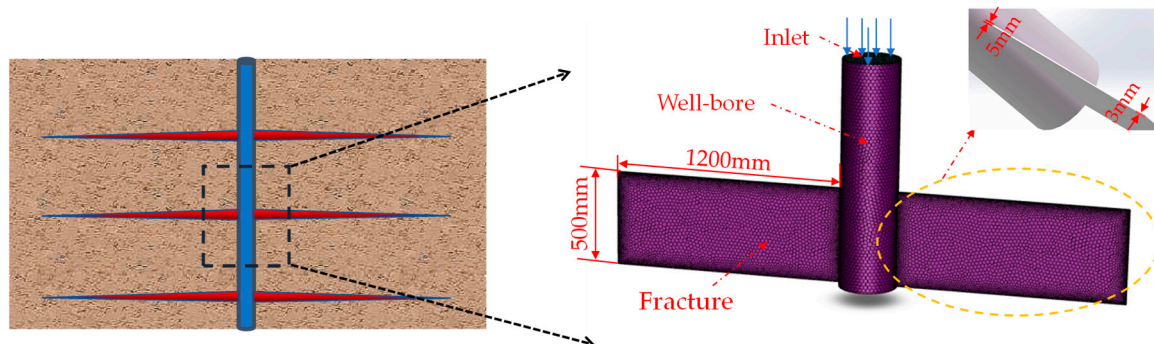


Figure 1. Wellbore fracture model.

In this model, the wellbore radius is 150 mm and the height is 1200 mm. On both sides of the wellbore are symmetrical ladder-shaped fractures with a length of 1200 mm and a height of 500 mm. The width of the fractures near the wellbore is 5 mm and that far from the wellbore is 3 mm. The minimum grid size is 0.5 mm, the maximum grid size is 20 mm, and the volume grid-filling method is poly-hexcore. The grid quality of all cells is above 0.7. The upper part of the wellbore is set as the pressure inlet, and the rest are set as the wall. Compared with the actual working condition, the model is small, and the fluid velocity changes greatly and is almost a straight line. Therefore, the laminar flow mode is adopted, and the time step is set as 0.01 s. Before simulation, the wellbore is fully filled with drilling fluid, and the fractures are fully filled with gas methane. The gas density is 0.2669 g/cm^3 , and the viscosity is $0.0361 \text{ mPa}\cdot\text{s}$. The density, viscosity, inlet pressure, fracture width, fracture height, and fracture length of the drilling fluid are changed to explore the effects of drilling fluid performance and fracture morphology changes. According to the gas invasion process, the dynamic image of the gas phase diagram over time is intercepted, which directly shows that the gas invasion process in the wellbore and the leakage process of the drilling fluid simulate the gas invasion law under different conditions. The specific parameters are shown in the table below.

Table 1. Analog input parameters.

Parameter	Gradient					
Viscosity of drilling fluid ($\text{mPa}\cdot\text{s}$)	10	20	30	40	50	
Drilling fluid density (g/cm^3)	1	1.2	1.8	2	2.4	
Inlet pressure (MPa)	0.5	1	1.5	2	2.5	
Fracture width (mm)	5–1	5–2	5–3	5–4	5–5	
Fracture length (mm)		600	1200	1800		
Fracture height (mm)	100	300	500	700	900	

3. Results and Discussion

Gas invasion in gas–liquid displacement generally occurs in vertically fractured reservoirs, and the safety density window of the reservoirs is generally narrow, even 0, which belongs to typical blowout leakage reservoirs of the same layer type. During the exploration and development of the reservoirs, a slightly higher drilling fluid density will lead to fracture opening and drilling fluid leakage, and a slightly lower drilling fluid concentration will lead to gas influx, which will lead to overflow, kick, and blowout. It is difficult to implement drilling using conventional drilling technology. In addition, this phenomenon

is difficult to identify in the initial detection, which can easily cause the phenomenon of “initial neglect, later difficult to deal with”, and even lead to serious downhole accidents.

The fundamental reason for gas invasion in gas–liquid displacement is that under near-equilibrium and overbalance conditions, annular drilling fluid leaks into the fracture under the effect of differential pressure, compressing the gas in the fracture, leading to the increase in gas pressure. When the gas pressure in the fracture increases to more than the annulus liquid column pressure, local negative pressure will be generated between them, forming gas intrusion.

3.1. Working Condition Simulation

The simulated wellbore has a diameter of 300 mm, a height of 1200 mm, a fracture height of 500 mm, a length of 1200 mm, and a fracture width of 5–3 mm. The volume fraction distribution of the gas invasion process is shown in Figure 2 (in the figure, the color represents the percentage content of gas in the fracture, the blue represents the volume fraction of 0, the red represents the volume fraction of 1, and the total volume fraction of the drilling fluid and gas is 1, so the deepest blue drilling fluid has the highest liquid-phase content). The wellbore pressure of the drilling fluid is 1 MPa, and the drilling fluid is based on the actual data on site, with a density of 1.2 g/cm^3 and a viscosity of $30 \text{ mPa}\cdot\text{s}$. The wellbore is full of drilling fluid, and the fractures are full of methane gas.

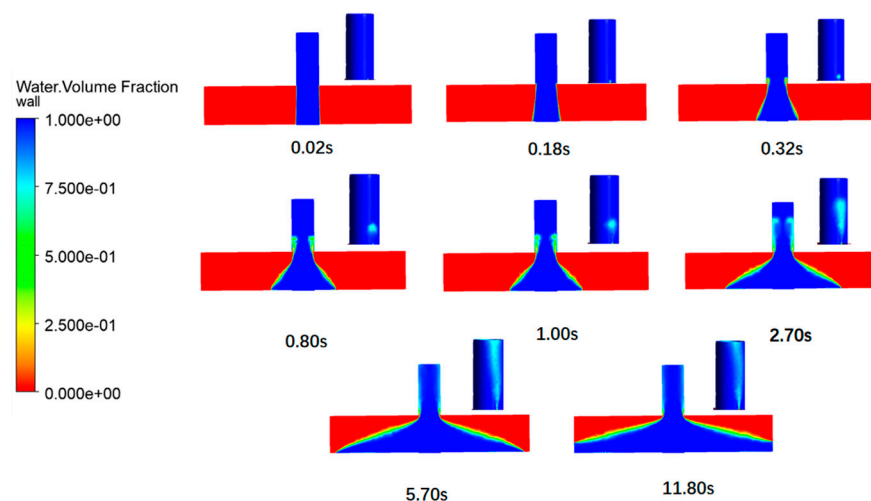


Figure 2. Gas invasion simulation volume fraction distribution.

Figure 2 shows the volume fraction distribution of the drilling fluid rapidly invading and occupying the fractures. The speed is fast in the first 1 s, and then the leakage of drilling fluid is slow; the pressure difference between the drilling fluid and gas decreases and gradually reaches equilibrium. The drilling fluid reaches half of the fracture capacity in about 5.7 s, the gas pressure in the fracture tends to be gentle, and the gas-phase velocity tends to be gentle at about 10 s. It can be observed from Figure 2 that the drilling fluid in the wellbore compresses the gas in the fracture with a pressure of 1 MPa. About 0.18 s later, the gas is extruded from the fracture and gradually rises along the inner wall of the wellbore to the wellhead. The migration rule of gas in the wellbore can be observed through the profile.

The pressure is recorded at the wellbore midpoint (0, 0, 450) and fracture midpoint (0, 160, 450) and the gas-phase velocity at the fracture midpoint. The velocity change is shown in Figure 3 and the pressure curve is shown in Figure 4. At the beginning, the pressure in the fracture and wellbore increases rapidly, and the pressure in the fracture exceeds the pressure in the wellbore. As the drilling fluid compresses the gas, the differential pressure between the fracture and the wellbore decreases. Until around 7 s, the differential pressure between the wellbore and the fracture is the smallest, and the pressure in the fracture is higher and lower than the pressure in the wellbore. This indicates that when the pressure in the wellbore and the fracture reaches a relative balance, gas invasion into the wellbore

occurs intermittently, and this process repeats endlessly. This can also be proven from the gas-phase fluid velocity diagram in Figure 3. At the beginning, the pressure difference between the two sides is large, and the gas velocity increases rapidly. The time taken is very short, about 0.12 s. With the differential pressure between the two sides decreasing, the gas-phase velocity gradually decreases, until about 7 s when the differential pressure reaches equilibrium, and the gas-phase velocity finally becomes stable.

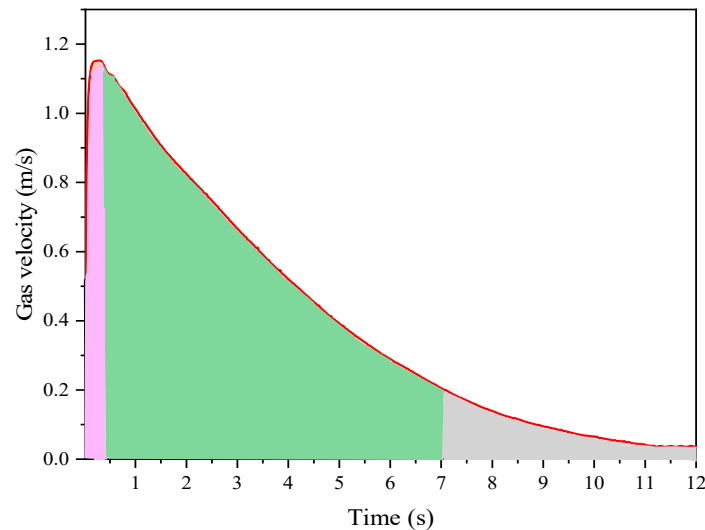


Figure 3. Velocity of gas phase.

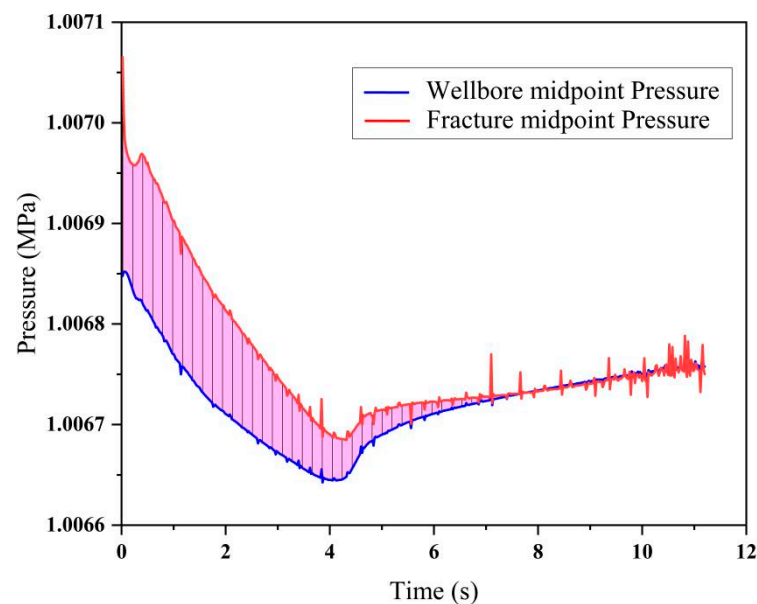


Figure 4. Pressure change of fracture and wellbore midpoint.

3.2. Factors Affecting Gas Invasion

According to the data analysis in the previous section, the constant-pressure drilling fluid flows into the fracture and compresses the gas in the fracture, causing the gas pressure to be higher than that of the drilling fluid in the wellbore, thus allowing the gas to enter the wellbore. The gas invasion velocity is affected by the drilling fluid characteristics, fracture morphology, wellbore pressure, and other aspects. Therefore, it is necessary to explore the influence of these factors on gas invasion.

3.2.1. Effect of Drilling Fluid Viscosity

In this simulation, the wellbore is 300 mm in diameter, 1200 mm in height, 500 mm in fracture height, 1200 mm in length, 5–3 mm in fracture width, 1.2 g/cm^3 in drilling fluid density, and 1 MPa in inlet pressure to explore the impact of different drilling fluid viscosities on gas invasion.

It can be seen from Figures 5 and 6 that the viscosity of the drilling fluid is proportional to the time required for gas–liquid displacement and gas invasion after the drilling fluid enters the fracture. The higher the viscosity of the drilling fluid, the longer the time it takes for the pressure in the fracture to rise to the effective fluid column pressure of the drilling fluid at the upper end of the fracture. With the increase in viscosity, the invasion rate of the gas decreases. This is because the greater the viscosity of the drilling fluid, the greater the flow resistance in the fracture, and the less drilling fluid will enter the fracture in a certain period of time, thus reducing the gas invasion velocity and delaying the time of gas invasion. During on-site construction, the viscosity of the drilling fluid can be properly increased to prevent gas invasion, but the viscosity should not be too high, as this will significantly reduce the drilling speed and reduce the service life of the mud pump. Therefore, the viscosity of the drilling fluid should be reasonably selected.

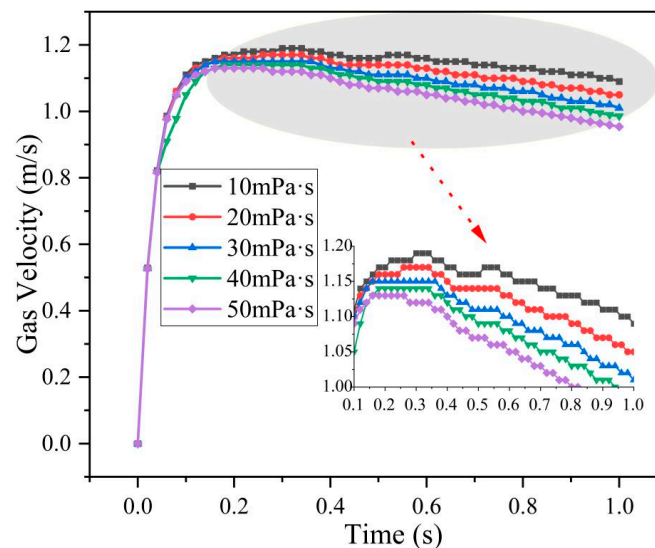


Figure 5. Gas-phase velocity under different drilling fluid viscosities.

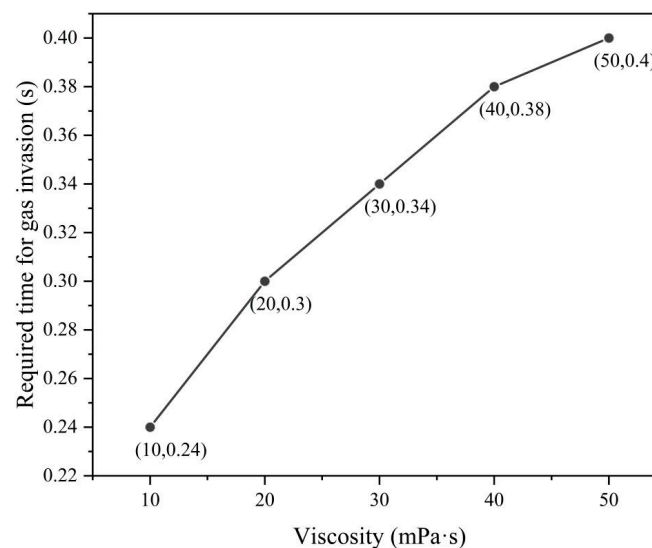


Figure 6. Time required for gas invasion under different drilling fluid viscosities.

3.2.2. Effect of Drilling Fluid Density

The simulated wellbore is 300 mm in diameter, 1200 mm in height, 500 mm in fracture height, 1200 mm in length, 5–3 mm in fracture width, 30 mPa·s in drilling fluid viscosity, and 1 MPa in initial wellbore pressure to explore the impact of different drilling fluid densities on gas invasion.

Figure 7 shows the pressure profile of the wellbore and fracture model when the gas influx occurs under different drilling fluid densities. It can be seen intuitively from the gas invasion pressure distribution that with the increasing density of the drilling fluid, the pressure distribution at each point when the gas influx occurs and the part with the largest pressure are distributed at the bottom of the model. The maximum pressure at 1 g/cm³ is 1.009 MPa; the maximum pressure is 1.011 MPa at 1.2 g/cm³; the maximum pressure is 1.018 MPa at 1.8 g/cm³; the maximum pressure is 1.020 MPa at 2 g/cm³; and the maximum pressure is 1.025 MPa at 2.4 g/cm³.

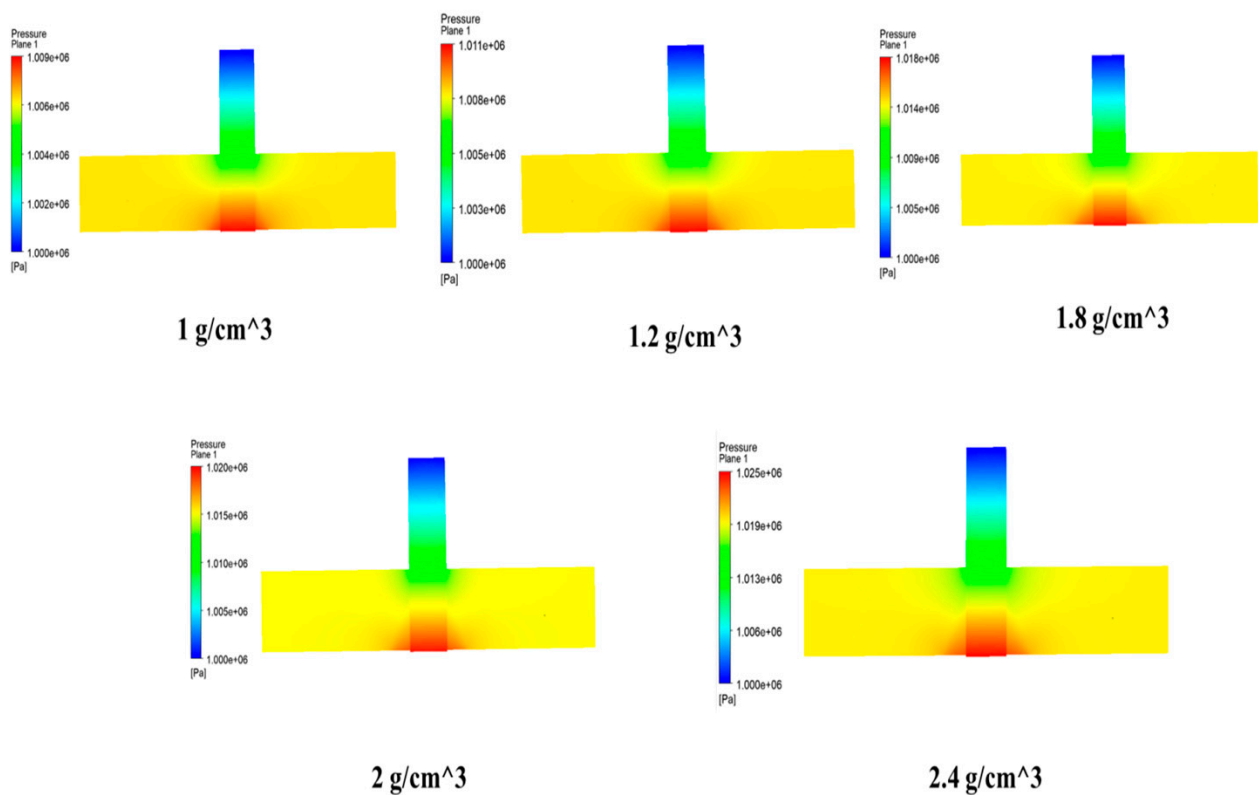


Figure 7. Gas invasion pressure distribution at different drilling fluid densities.

This makes the gas velocity at a point (0,160,450) in the fracture in Figure 8 increase with the increase in drilling fluid density. When the drilling fluid density is below 1.2 g/cm³, the maximum gas invasion velocity is less than 1.2 m/s; when the drilling fluid density is more than 1.2 g/cm³, the maximum gas invasion velocity is more than 1.6 m/s. It can be seen intuitively from Figure 9 that with the increasing density of the drilling fluid, the fluid continuously enters into the fracture, squeezing the gas in the fracture, and the time required for gas invasion gradually decreases. This is because when density of the drilling fluid increases, the corresponding hydrostatic column pressure of the fluid in the wellbore increases. The drilling fluid has a stronger impact on the gas in the fracture, and the drilling fluid enters the fracture at a faster speed. In the same fracture model, it takes less time to squeeze the gas in the fracture to raise it to the same pressure range. The change in the drilling fluid density is positively correlated with the change in the gas invasion velocity. When gas influx is encountered during drilling or production, the density of the drilling fluid can be appropriately reduced to delay the occurrence of this phenomenon, and win time for well control.

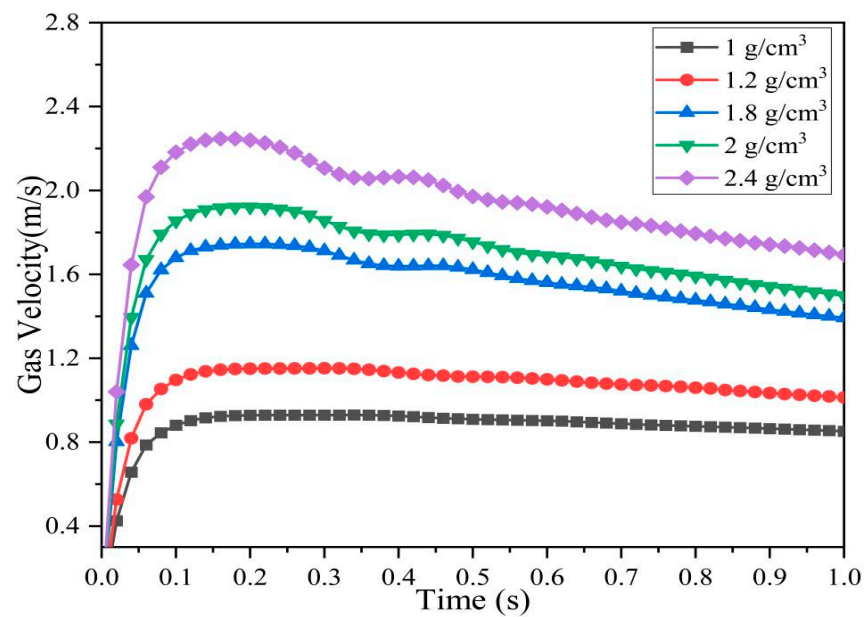


Figure 8. Velocity of a point in the fracture under different drilling fluid densities.

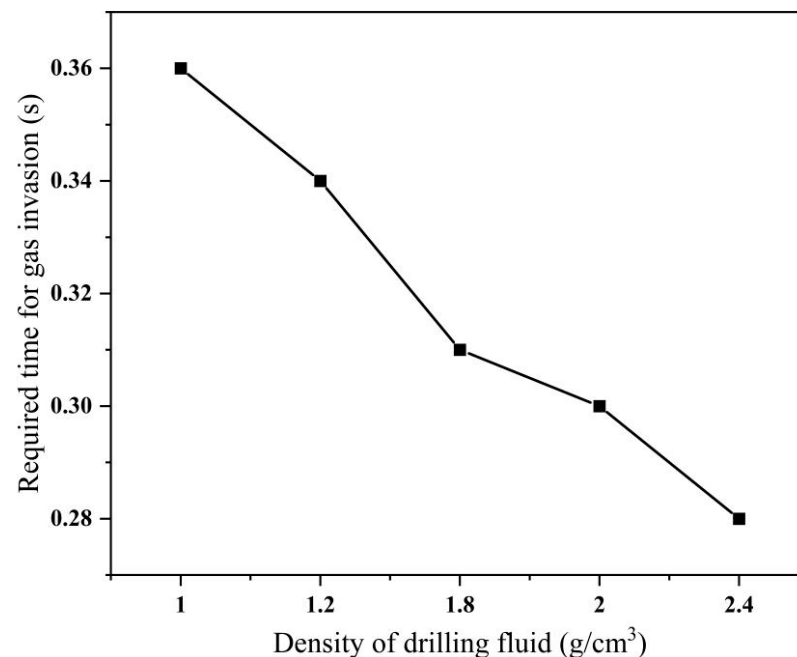


Figure 9. Time required for gas invasion under different drilling fluid densities.

3.2.3. Effect of Pressure Difference

In this simulation, the wellbore is 300 mm in diameter, 1200 mm in height, 500 mm in fracture height, 1200 mm in length, 5–3 mm in fracture width, 30 mPa·s in drilling fluid viscosity, and 1.2 g/cm³ in drilling fluid density to explore the impact of different inlet pressures on gas invasion.

It can be seen from Figure 10 that the influence of the wellbore inlet pressure on gas–liquid displacement in fractures is weak. The inlet pressure is within 0.5–2.5 MPa, and the time required for gas invasion is mostly kept between 0.33–0.34 s. When the drilling fluid enters the wellbore at a lower pressure through the inlet, the drilling fluid compresses the gas in the fracture. When gas invasion occurs, the pressure of the gas in the fracture must be greater than the “barrier pressure” formed by the static fluid column in the wellbore. When the drilling fluid enters the wellbore at a higher pressure through the

inlet, the drilling fluid has a strong impact on the fracture. However, if gas invasion occurs, the gas pressure must be greater than the “pressure barrier” of the wellbore’s static liquid column at this time.

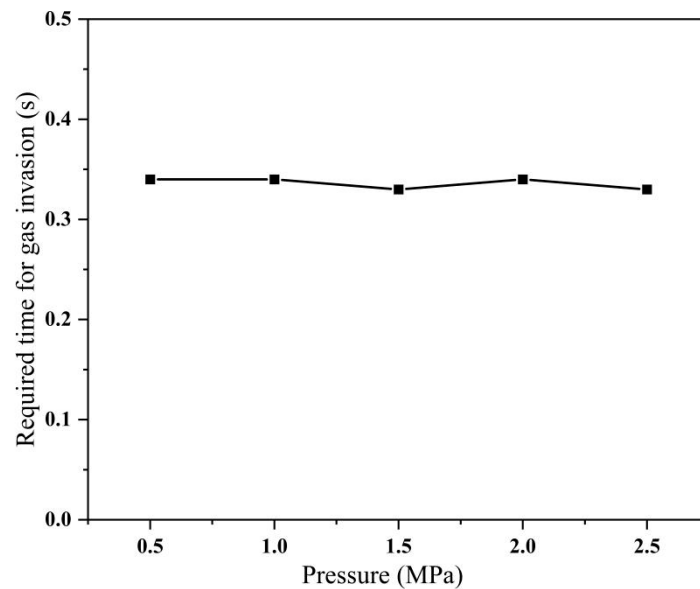


Figure 10. Time required for gas invasion under different pressures.

Figure 11 reflects the curve of gas velocity change with time at a point (0,160,450) in the fracture. It can be seen from the figure that the gas velocity change is basically independent of the inlet pressure, that is, the greater the inlet pressure, the greater the hydrostatic column “barrier pressure”, the smaller the inlet pressure, and the smaller the hydrostatic column “barrier pressure”.

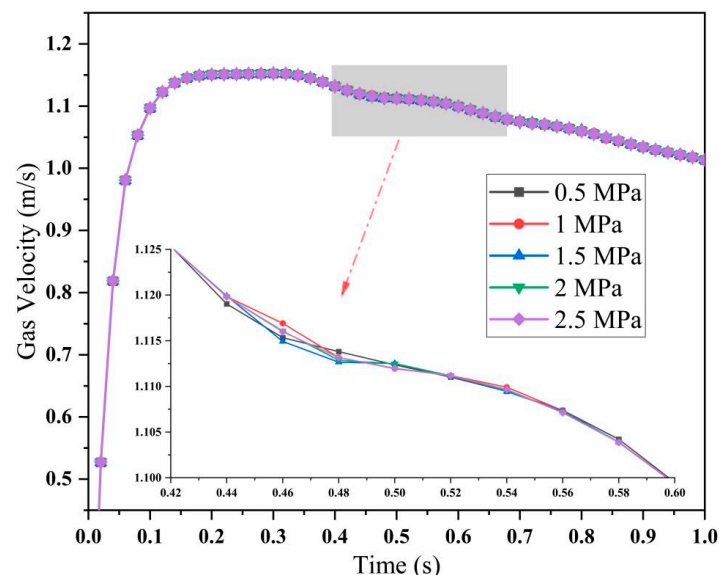


Figure 11. Velocity of a point in the fracture under different pressures.

3.2.4. Effect of Fracture Width

The simulated wellbore adopts a diameter of 300 mm, a height of 1200 mm, a fracture height of 500 mm, a length of 1200 mm, an inlet pressure of 1 MPa, a drilling fluid viscosity of 30 mPa·s, and a drilling fluid density of 1.2 g/cm³ to explore the impact of different fracture widths on gas invasion.

It can be seen from Figure 12 that the time required for gas invasion in gas–liquid displacement is negatively correlated with the fracture width. The time for gas invasion in the 5–1 mm wide fracture is 0.39 s, while the time for gas invasion in the 5–5 mm wide fracture is 0.26 s, which indicates that the fracture width has a great influence on gas invasion in gas–liquid displacement.

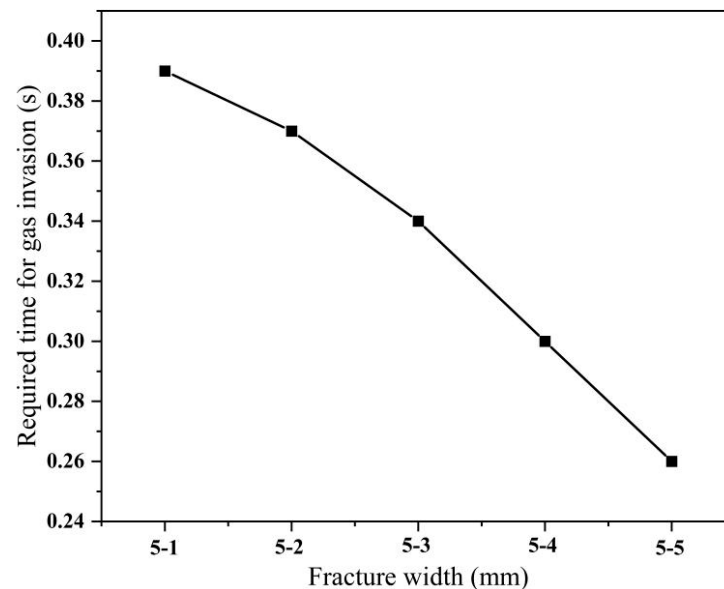


Figure 12. Time required for gas invasion under different fracture widths.

Because the time for gas invasion of the above-mentioned fractures is less than 0.4 s, Figure 13 shows the morphological distribution of the gas and liquid phases in the wellbore and fractures at 0.4 s of five fracture widths. With the increase in the fracture width, the volume occupied by the liquid phase in the model becomes larger and larger, and the volume of the gas phase entering the wellbore also increases [29]. This is because a fracture with larger width has less flow resistance. The drilling fluid can easily enter the fracture and squeeze the gas. The “barrier pressure” of the wellbore is the same. The fluid with smaller flow resistance has a stronger impact on the gas in the fracture, and it is easier for the gas to enter the wellbore. The velocity at a point (0,160,450) in the fracture in Figure 14 also proves the previous viewpoints. The wider the fracture, the smaller the fluid resistance and the greater the gas flow velocity. This also provides a solution to prevent gas invasion. The key to effectively reducing gas invasion is to use appropriate plugging particles, change fractures into holes, change holes into gaps, and reduce the width of the fractures.

3.2.5. Effect of Fracture Height

The simulated wellbore has a diameter of 300 mm, a height of 1200 mm, a fracture width of 5–3 mm, a length of 1200 mm, an inlet pressure of 1 MPa, a drilling fluid viscosity of 30 mPa·s, and a drilling fluid density of 1.2 g/cm³. The impact of different fracture heights on gas invasion is explored. The results are shown in the following figure.

Figure 15 shows the time required for gas invasion at different fracture heights. The lower the fracture height, the easier it is for the gas invasion to occur, and the impact will be more obvious. With the increase in the height, the time for gas invasion will gradually flatten, and the time for gas invasion to occur in the 700 mm high fracture and 900 mm high fracture is 0.36 s. With the increase in the fracture height, the time for gas invasion will not be extended. However, under the same conditions, the higher the fracture height, the larger the fracture volume. Once the gas is squeezed, its flow resistance is smaller and the flow speed is larger, as shown in Figure 16.

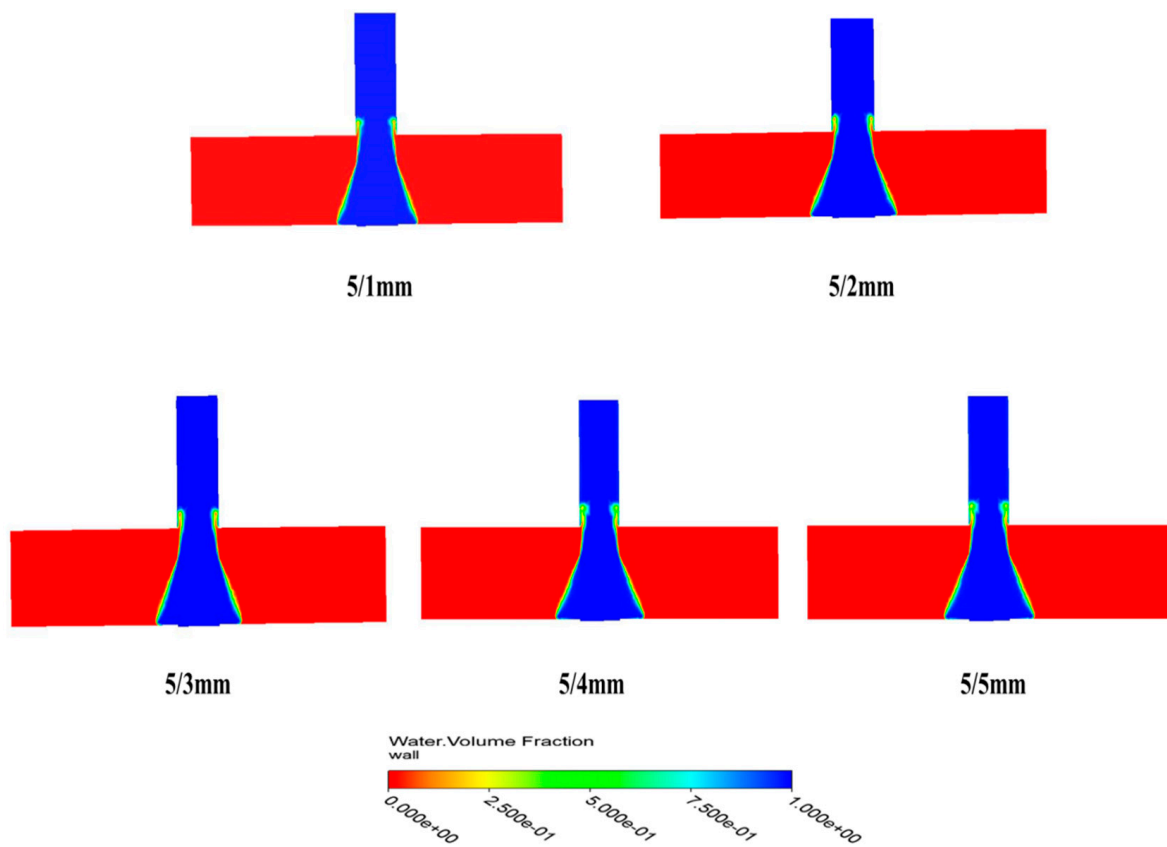


Figure 13. Volume fraction distribution of gas-liquid two-phase flow with different fracture widths at 0.4 s.

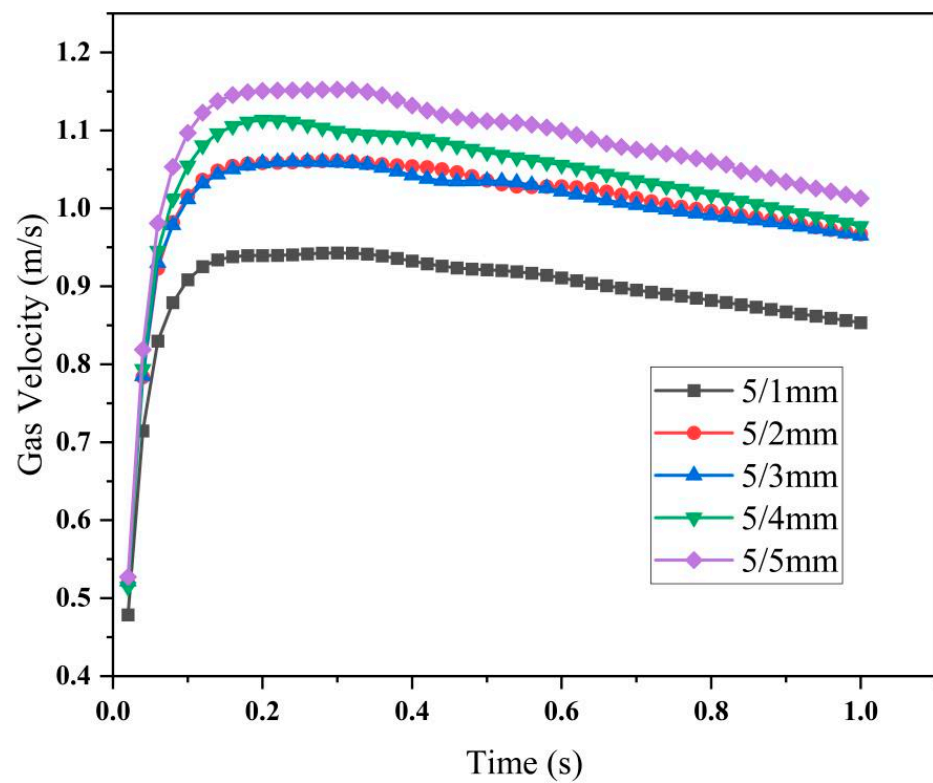


Figure 14. Velocity of a point in a fracture with different fracture widths.

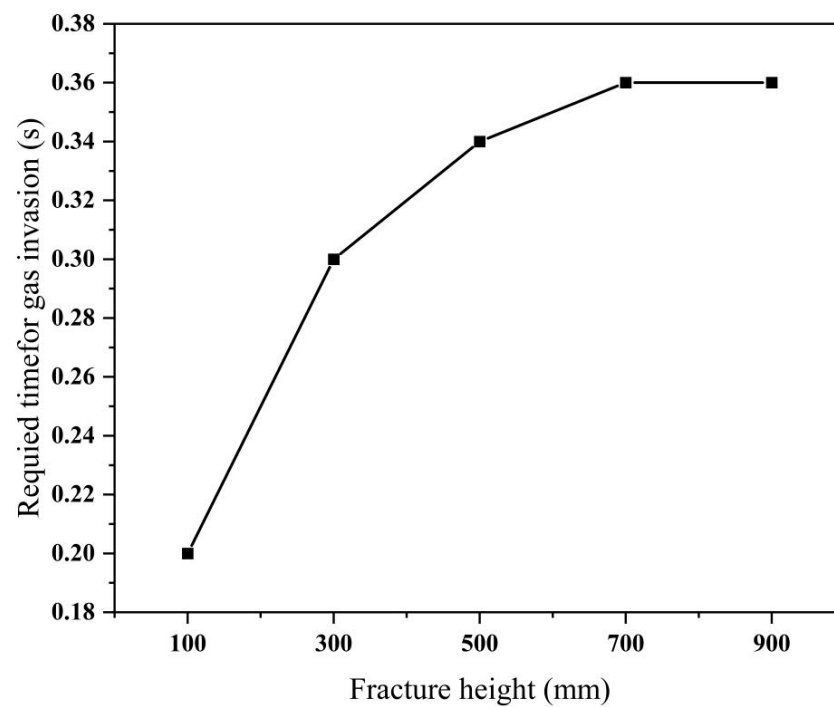


Figure 15. Time required for gas invasion at different fracture heights.

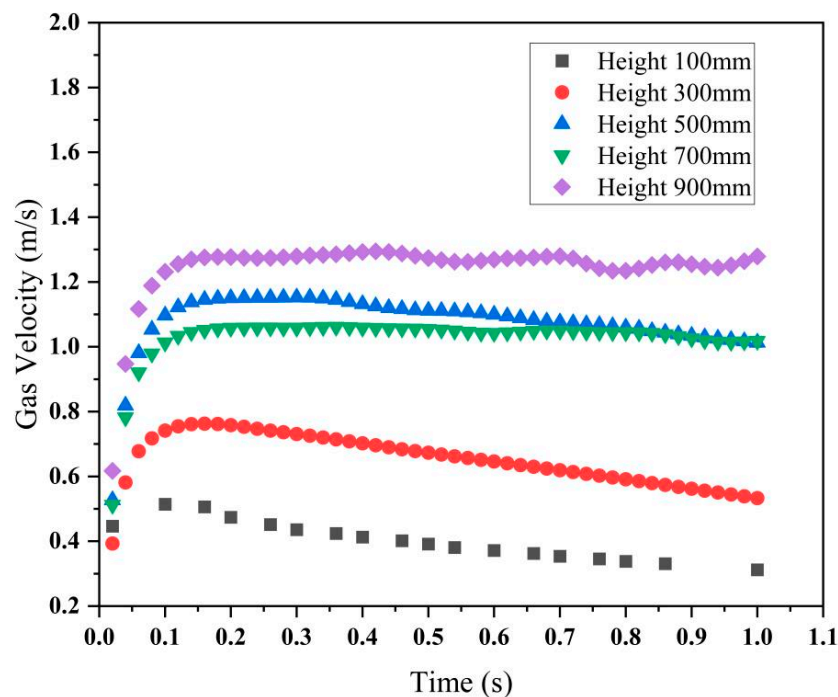


Figure 16. Velocity of a point in a fracture at different fracture heights.

3.2.6. Effect of Fracture Length

The diameter of the simulated wellbore is 300 mm, the fracture width is 5–3 mm, the length is 1200 mm, the height is 500 mm, the inlet pressure is 1 MPa, the viscosity of the drilling fluid is 30 mP·s, and the density of the drilling fluid is 1.2 g/cm³. The impact of different fracture lengths on gas invasion is explored, and the results are shown in the following figures.

It can be seen from Figure 17 that there is a negative correlation between the time required for gas invasion and the length of the fractures. The length of the fracture has

obvious influence on gas invasion in gas–liquid displacement. The longer the fracture, the more difficult it is for gas invasion to occur. This is because under the same conditions, the longer the fracture, the greater the resistance along the fracture, the longer the drilling fluid enters the fracture, and the longer the time taken to reach the “barrier pressure”, that is, the longer the time taken to start the gas–liquid displacement of the gas invasion. Figure 18 shows the velocity distribution at 0.5 s under each fracture. The longer the fracture, the harder it is for the drilling fluid to enter the fracture to squeeze the gas. Under the same conditions, the shorter the fracture, the more the drilling fluid enters the fracture, and the easier it is for the gas to be squeezed out.

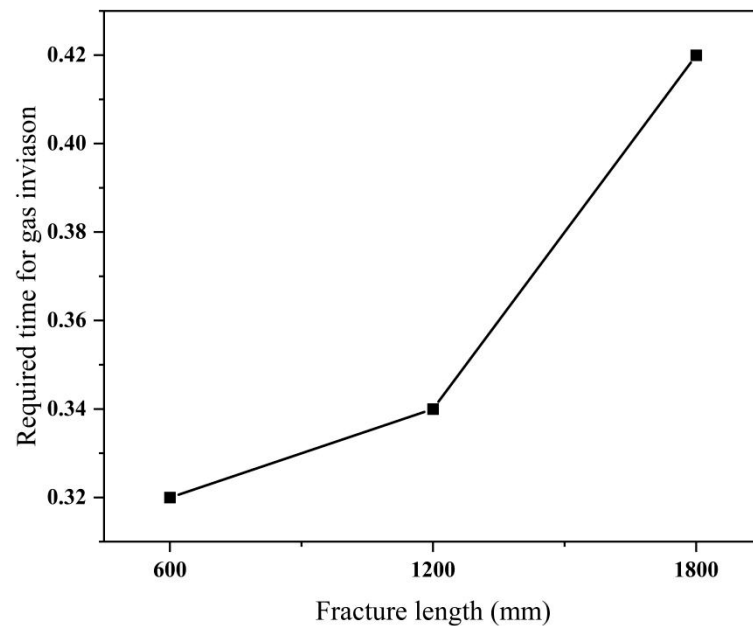


Figure 17. Time required for gas invasion under different fracture lengths.

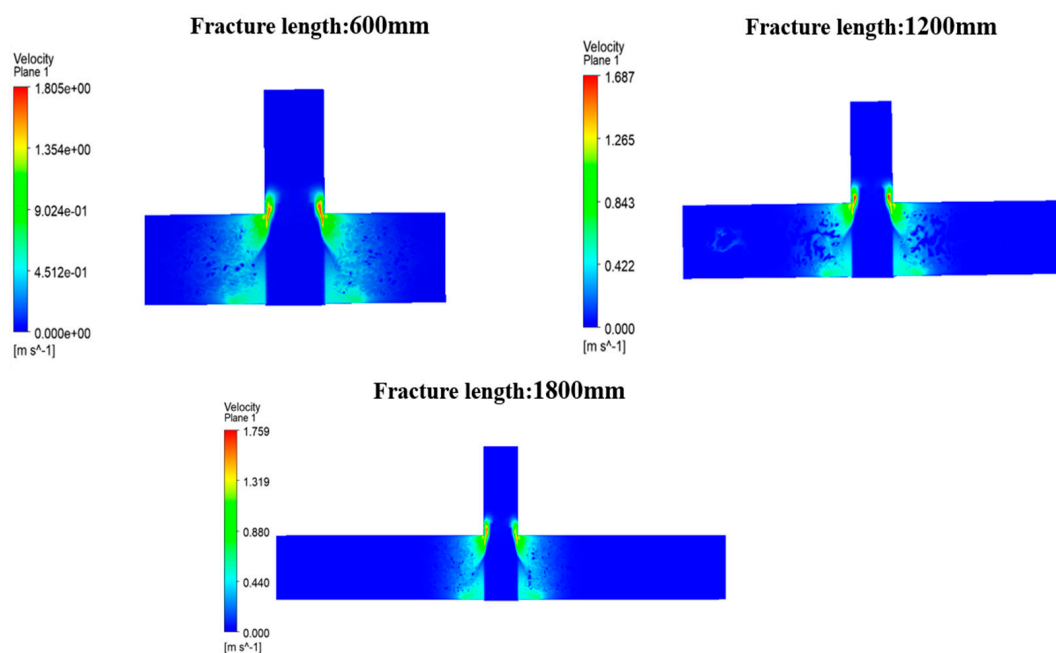


Figure 18. Velocity distribution at different fracture lengths in 0.5 s.

4. Conclusions

1. Gas–liquid displacement gas invasion occurs intermittently. When the gas pressure in the fracture is close to the wellbore pressure, the gas pressure in the fracture rises and falls around the wellbore pressure. The amount of gas being squeezed out is small and not easy to see.

2. The viscosity of the drilling fluid mainly affects the occurrence of gas invasion through flow resistance. The higher the viscosity, the less likely it is that the gas invasion will occur, but the viscosity has no obvious effect on the gas invasion. The change in the drilling viscosity on the gas invasion velocity is small when it gradually increases from 10–50 mPa·s, all within 1.0–1.2 m/s. The density of the drilling fluid mainly affects the gas invasion phenomenon by changing the pressure distribution in the wellbore, and the change in the density is positively correlated with the occurrence time of the gas invasion. The inlet pressure has the least significant effect on the occurrence of gas invasion: the pressure gradually increases from 0.5–2.5 MPa, and the occurrence time of the gas invasion is always about 0.35 s.

3. The influence of fracture morphology is very obvious for gas invasion. The fracture morphology mainly affects the occurrence of gas invasion through the resistance of the fluid along the fracture. The longer the fracture, the less likely it is to for gas invasion to occur. Similarly, the wider the fracture, the less likely it is to experience gas invasion. The influence of fracture height on gas invasion is different from the former. The height is 300–700 mm. With the increase in the fracture height, the time required for gas invasion is longer. When the height is 700–900 mm, the time required for gas invasion is basically unchanged with the increase in the height.

Author Contributions: Conceptualization, C.Y. and J.G.; methodology, C.Y. and K.L.; software, C.Y.; validation, C.Y., J.P. and S.X.; formal analysis, P.X.; investigation, C.Y. and K.L.; resources, S.X.; data curation, P.X.; writing—original draft preparation, C.Y.; writing—review and editing, C.Y.; visualization, J.G.; supervision, J.P.; project administration, C.Y.; funding acquisition, C.Y. All authors have read and agreed to the published version of the manuscript.

Funding: The authors gratefully acknowledge the financial support from the major engineering technology field test of China National Petroleum Corporation’s “Integration and Test of Excellent and Fast Drilling and Completion Technology in Key Areas such as the Southern Margin of Junggar and Mahu” (No. 2019F-33) and the National Natural Science Foundation of China (No. 51804044).

Institutional Review Board Statement: Not applicable.

Informed Consent Statement: Written informed consent has been obtained from the patient(s) to publish this paper.

Data Availability Statement: Data available on request due to restrictions eg privacy or ethical. The data presented in this study are available on request from the corresponding author.

Conflicts of Interest: No conflict of interest exists in the submission of this manuscript, and all authors approve the manuscript for publication. I want to declare on behalf of my co-authors that the work described is original research that has not been published previously and is not under consideration for publication elsewhere, in whole or in part. All of the authors listed have approved the manuscript.

References

1. Lin, A.C.; Han, L.X. Interpretation of runaway blowout in well LuoJia 16—Well control problem in overbalanced drilling. *Drill. Prod. Technol.* **2006**, *29*, 3.
2. Li, Y.; He, M.; Xia, W.; Li, X. Study on swelling and migration law of dissolved gas during gas kick of oil-based drilling fluid in horizontal well. *China Saf. Prod. Sci. Technol.* **2016**, *12*, 6.
3. Gravdal, J.E.; Nikolaou, M.; Breyholtz, Ø.; Carlsen, L.A. Improved kick management during MPD by real-time pore-pressure estimation. *SPE Drill. Complet.* **2010**, *25*, 577–584. [[CrossRef](#)]
4. Rommetveit, R.; Vefring, E.H. CoMParison of Results from an Advanced Gas Kick Simulator with Surface and Downhole Data from Full Scale Gas Kick Experiments in an Inclined Well. In Proceedings of the SPE Annual Technical Conference and Exhibition, Dallas, TX, USA, 6–9 October 1991.

5. Baoping, L.U.; Hou, X.; Xing, S. Asphalt Displacement Mechanism and Pore Pressure Fluctuation in Yadavaran Oilfield, Iran. *J. China Univ. Pet.* **2017**, *41*, 88–93.
6. Louis, C.; Maini, Y.N. Determination of in-situ hydraulic parameters in jointed rock. *Int. Soc. Rock Mech. Proc.* **1970**, *1*, 1–19.
7. Majidi, R.; Miska, S.Z.; Yu, M.; Thompson, L.G.; Zhang, J. Quantitative Analysis of Mud Losses in Naturally Fractured Reservoirs: The Effect of Rheology. *SPE Drill. Complet.* **2010**, *25*, 509–517. [[CrossRef](#)]
8. Zhang, Y.; Zhao, W.; Zhang, X.; Li, S. Movement features of gas in different types of drilling fluid during kicking in deepwater wells. *Oil Drill. Prod. Technol.* **2016**, *38*, 5.
9. Gugl, R.; Kharrat, R.; Shariat, A.; Ott, H. Evaluation of Gas-Based EOR Methods in Gas-Invaded Zones of Fractured Carbonate Reservoir. *Energies* **2022**, *15*, 4921. [[CrossRef](#)]
10. Gandomkar, A.; Nasriani, H.R.; Enick, R.M.; Torabi, F. The effect of CO₂-philic thickeners on gravity drainage mechanism in gas invaded zone. *Fuel* **2023**, *331*, 125760. [[CrossRef](#)]
11. Cheraghian, G.; Rostami, S.; Afrand, M. Nanotechnology in enhanced oil recovery. *Processes* **2020**, *8*, 1073. [[CrossRef](#)]
12. Shen, J.; Du, Z.; Li, H.; Li, L.; Wang, F.; Ni, J.; Teng, G. Fracture gas invasion mechanism and plugging method of shale gas layer. *J. Chengdu Univ. Technol.* **2022**, *5*, 579–585.
13. Biao, Q.; Junwei, F.; Lixin, Z.; Shengming, H.; Jun, Z.; Wei, H. Simulation of the lost circulation in fractured formation under the gas invasion conditions. *Sci. Technol. Eng.* **2021**, *17*, 7059–7066.
14. Jiang, R.; Cui, Y.; Zhang, C.; Chen, X. Numerical simulation of cuttings transport during gas invasion in eccentric horizontal Wells of shale gas. *Technol. Ind.* **2022**, *6*, 283–289.
15. Liu, F.; Cheng, C.; Qiao, S.; Xing, X.; Wu, Y.; Yang, H. Transient changes of annulus pressure at the initial stage of gas influx. *Drill. Prod. Technol.* **2022**, *2*, 1–7.
16. Yue, H.; Wu, P.; Liang, J.; Zhong, C.; Zhang, Z.; Li, Z.; Li, H. Gas-liquid gravity displacement laws of horizontal during well drilling in shale formations with developed fractures. *Nat. Gas Ind.* **2021**, *12*, 90–98.
17. Wang, J.; Li, J.; Liu, G.; Luo, X. Study on the change law of annular outlet flow rate in new-type of dual-gradient drilling under gas cut condition. *Pet. Drill. Tech.* **2020**, *4*, 43–49.
18. Huang, G.; He, S.; Tang, M.; Liu, Y.L. A study on the effect of displacement gas cut on fractured reservoirs in Shunnan Block. *Pet. Drill. Tech.* **2018**, *5*, 21–25.
19. Zhao, Z.; Pu, X.; Wang, G.; Li, Z.; Chen, L.; Cao, C. Numerical study of the gas-fluid displacement invasion behavior in a fractured carbonate reservoir. *J. Nat. Gas Sci. Eng.* **2015**, *27*, 686–691. [[CrossRef](#)]
20. Bennion, D.B.; Lunan, B.; Saponja, J. Underbalanced drilling and completion operations to minimize formation damage-reservoir screening criteria for optimum application. *J. Can. Pet. Technol.* **1998**, *37*, 9. [[CrossRef](#)]
21. Nickens, H.V. A dynamic computer model of a kicking well. *SPE Drill. Eng.* **1987**, *2*, 159–173. [[CrossRef](#)]
22. Zhang, X.; Zhou, Y.; Liu, W.; Guo, Q.; Cui, T. Characters of gravity replacement gas kick in carbonate formation. *Acta Pet. Sin.* **2014**, *35*, 958–962.
23. Zhang, X.; Zhou, Y.; Liu, W.; Guo, Q. A method for characterization and identification of gas kicks caused by underbalanced pressure and gravity displacement. *J. China Univ. Pet.* **2015**, *39*, 95–102.
24. Hou, X.; Zhao, X.; Meng, Y.; Yang, S.; Li, G.; Liu, W. Liquid-Liquid Gravity Displacement Test Based on Experimental Apparatus for Real Fractures. *Pet. Drill. Tech.* **2018**, *1*, 30–36.
25. Fang, J.; Zhu, L.; Luo, F.; Zhang, J.; Wang, Y.; Huang, W.; Niu, X. Simulation study on the effects of drilling fluid on gas invasion from fractured formations. *Drill. Complet. Fluid* **2019**, *3*, 287–292.
26. Shu, G.; Meng, Y.; Li, G.; Wei, N.; Zhao, X.; Yang, M. Mechanism of mud loss and well kick due to gravity displacement. *Pet. Drill. Tech.* **2011**, *1*, 6–11.
27. Zhao, X.; Hou, X.; Yang, S.; Bao, H. Pattern and control of gravity displacement between asphaltic heavy oil and drilling fluid. *Oil Drill. Prod. Technol.* **2016**, *38*, 622–627.
28. Song, R.; Sun, B.; Liu, X.; Wang, Z. Calculation and analysis of bottom hole pressure in wellbore after gas invasion. *Duankuai Youqitian Fault Block Oil Gas Field* **2011**, *4*, 486–488.
29. Li, Z. The Vertical Cracks Formation Gas Liquid Displacement and Prevent Gas Invasion Drilling Fluid Plugging Technology Research. Master's Thesis, Southwest Petroleum University, Chengdu, China, 2014. Available online: <https://kns.cnki.net/KCMS/detail/detail.aspx?dbname=CDFDLAST2015&filename=1014419528.nh> (accessed on 10 September 2022).